



Regional changes of climate extremes and its effect on rice yield in Jiangsu province, southeast China

Jin Huang^{1,2} · Fangmin Zhang¹ · Limin Zhou¹ · Zhenghua Hu^{1,2} · Ying Li³

Received: 3 May 2017 / Accepted: 29 January 2018 / Published online: 6 February 2018
© Springer-Verlag GmbH Germany, part of Springer Nature 2018

Abstract

In this study, the regional variations of climate extremes and its possible impact on rice yield in Jiangsu province, southeast China were investigated. A total of 18 climate extremes indices (CEI) of rice-growing period (May–October) based on the daily climate records and rice yield data at 52 stations during 1961–2012 were calculated and analyzed. The main findings were as follows: (1) due to the remarked regional differences of climate extremes, Jiangsu could be divided into six climatic subregions: westernmost, northwest, north, southwest, south, and southeast corner; (2) trends of 18 indices in the six subregions using Mann–Kendall test indicated that Jiangsu was dominated by an obvious wetting and warming tendency, especially in the southern area; (3) correlation analysis between rice yield and CEI using first-difference and climate-induced yield method showed that the negative influences of precipitation extremes were more notable compared to temperature extremes; (4) P95 [precipitation due to very wet days (> 95th percentile)] should be selected as a key meteorological disasters indicator affecting rice yield in the northwest, north, southwest, and south Jiangsu; (5) the increase of P95 since 1990s was detected in most of Jiangsu, which would bring huge risks to rice growing.

Keywords Climate extremes · Rice yield · Jiangsu

Introduction

Excessive increase in greenhouse gas emitted by human activities will continue aggravating global warming, which would intensify the climate extremes in recent decades (Sun et al. 2013). The impacts of climate extremes varied and acted on many aspects, ultimately affecting our capacity to provide food and water security, protect human health and

Earth's ecosystems (Rummukainen 2013; Sun et al. 2015; Liu et al. 2016a). With the recent development for defining climate extremes, Expert Team on Climate Change Detection and Indices (ETCCDI) released by the CCI/CLIVAR/JCOMM has been widely used for investigating the changes in climate extremes at different timescales around the world (Wang et al. 2016). On the basis of ETCCDI, previous study indicated that climate extremes had exhibited the significant changes in Asia, which would have a wide range impacts on crop production (Lee et al. 2012).

Rice (*Oryza sativa* L.) is one of the most important food source of more than half of the world's population, and Asia is the world's most important growing area (Sawano et al. 2015). In Asia, studies on the responses of rice yield to climate extremes using the climate indices defined by ETCCDI had attracted widespread concern. The correlation analysis by Revadekar and Preethi (2012) revealed that a large part of India exhibited a positive relationship between kharif rice yield and moderate, heavy and very heavy rainfall events. In Pakistan, the high-temperature stress had negative effect on rice yield, while the cumulative rainfall had positive effect on rice yield (Arshad et al. 2017). As for Bangladesh, rice yield showed a negative correlation with high-temperature

✉ Fangmin Zhang
nfuecology@aliyun.com

¹ Collaborative Innovation Center on Forecast and Evaluation of Meteorological Disasters/Jiangsu Key Laboratory of Agricultural Meteorology, Nanjing University of Information Science and Technology, Nanjing 210044, China

² Jiangsu Collaborative Innovation Center of Atmospheric Environment and Equipment Technology (CICAEET), Nanjing University of Information Science and Technology, Nanjing 210044, China

³ China Meteorological Administration/Henan Key Laboratory of Agrometeorological Support and Applied Technique, Henan Institute of Meteorological Sciences, Zhengzhou 450003, China

events and heavy rainfall during the growing periods (Ara et al. 2016). In China, lots of studies had been mainly focused on the responses of rice yield to normal climate variables (e.g., annual precipitation, average temperature) (Quan et al. 2013). However, investigations on the relationship between rice yield and climate extremes indices were still very few.

Located in the mid-lower Yangtze River basin of southeast China, Jiangsu province displays a vital role in the country's economic development and agro-environmental conservation. Jiangsu has been always ranked the top five provinces in rice production in China, and it is one of the three major grain net exportation provinces in south China, which plays an important role in rice productivity from country's food security perspective (Huang et al. 2016a). However, the comprehensive investigations on the spatial and temporal variability of climate extremes in Jiangsu were not reported. Thus, the objective of this paper is to investigate the regional differences of climate extremes across Jiangsu using the multi-indices recommend by ETCCDI, and further the possible impacts of climate extremes on rice yield were also discussed. All this may help us to better understand response of rice yield to climate changes and should be beneficial to the grain production safety in Jiangsu.

Study area and data

The study site (Jiangsu province) located in southeast China which is positioned between 116°E–122°E latitude and 30°N–36°N longitude, along the southern bank of the mid-lower Yangtze River basin. Jiangsu is situated in

a transitional zone between temperate zone and subtropical zone. Within the province, there are two typical climate types: the humid subtropical monsoon climate in the southern area of Jiangsu, and the cool and temperate continental monsoon climate, to the north of the old Huai River. Between spring and summer, the south receives prolonged rains of summer-monsoon origin. The northeastern coast is often visited by destructive typhoons between late summer and early autumn. In this province, the single season cropping of rice from May to October is the main planting system.

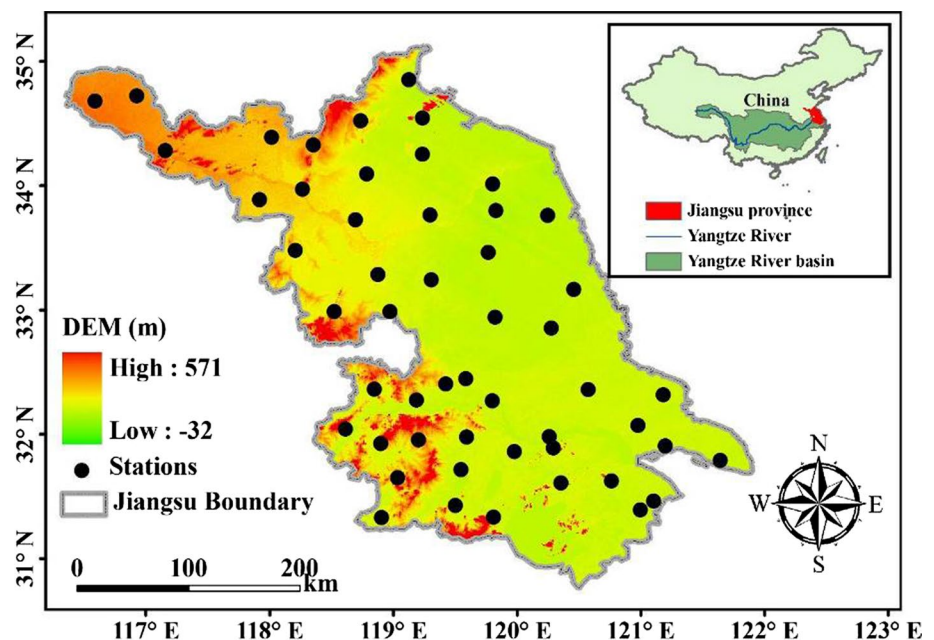
The data of daily precipitation, daily maximum temperature (TX), and daily minimum temperature (TM) in 52 meteorological stations across Jiangsu province during the period of 1961–2012 were obtained from the Meteorological Bureau of Jiangsu Province (MBJP). The preprocessing of climate data was applied using the RHtestsV4 software package which was developed by Wang and Feng (2013). Daily climate data in each station pass the homogeneity test which is plotted in Fig. 1. Additionally, the total yield data of single cropping rice for 52 years (1961–2012) in 52 producing zones corresponding to the stations listed in Fig. 1 were collected from the Statistical Bureau of Jiangsu Province (SBJP).

Methods

Climate extremes indices (CEI)

A set of climate indices have been defined by the ETCCDI (http://etccdi.pacificclimate.org/list_27_indices.shtml) and

Fig. 1 Meteorological stations with DEM distribution used in this study and location of Jiangsu province, China



these indices are frequently used to depict climate extremes in the recent decades. Among them, 18 extreme climate indices (CEI) listed in Table 1 were used. All the CEI were derived from daily climate data at the time scale of rice-growing period (May–October).

Climatic regionalization

Principal component analysis (PCA) cooperatively with K-means cluster analysis (KCA) is often used for identifying homogenous climate subregions (Huang et al. 2016b). R-mode PCA (data matrix with variables vs. stations) can reveal the interaction among the variables studied, and decompose excessive variables into few of new uncorrelated indicators named principal components. KCA is frequently used to cluster the neighboring meteorological stations into homogeneous and distinct groups having members with similar climate features (Sönmez and Kömüscü 2011). The silhouette coefficient (*S*) is often used to check the success of cluster assigning (Kaufman and Rousseeuw 1990), and it can be calculated as the following equation:

$$S(i) = \frac{\min(b(i, k)) - a(i)}{\max\{a(i), \min(b(i, k))\}}$$

where *a(i)* is the average distance of *i*th sample from the other members in the same cluster, and *b(i, k)* is the average distance of the *i*th sample from the members of the *k*th

cluster. The *S* ranges from − 1 to + 1, and the higher the *S* value indicates a better classification. The optimal classification number is obtained when the average of *S* reaches a maximum and the negative *S* value reaches a minimum (Liu et al. 2016b). The subregional time series of rice yield and CEI were calculated as the arithmetic mean at stations of each cluster identified using KCA.

Response of rice yields to CEI

Before estimating the effects of extreme climate events on rice yield, the influences of possible confounding non-climatic factors should be removed using the first-difference or climate-induced yield method (Yang et al. 2015). As for first-difference method, we computed the first-difference time series (i.e., the difference in values from the current year to the next) for rice yield (Δ Yield) and Δ CEI, and then the relationships between Δ Yield and Δ CEI were evaluated using Pearson correlation analysis method. In the climate-induced yield method, the actual crop yield can be equal to the sum of management-induced yield and climate-induced yield (EI-Maayar and Lange 2013). The management-induced yield is the fitting results from the actual yield series using linear or nonlinear fitting equations. In Jiangsu, 5-year moving average function had been proved to be effective in modeling the management-induced yield of rice (Huang et al. 2016a). The Pearson correlation between

Table 1 Definition of climate extremes indices used in this study

Name	Definition of climate extremes indices	Units
TP	Total precipitation amount in rainy days	mm
DR	Number of rainy days	days
D25	Number of days when daily precipitation \geq 25 mm (heavy rain)	days
D50	Number of days when daily precipitation \geq 50 mm (rainstorm)	days
MP1d	Maximum 1-day precipitation	mm
MP7d	Maximum 7-day precipitation	mm
CWD	Maximum number of consecutive rainy days	days
P95	Total precipitation when daily precipitation > 95th percentile of precipitation on rainy days in the 1961–1990 period	mm
TXx	Warmest day, the highest TX	°C
TXm	Coldest day, the lowest TX	°C
TX10	Cold days, when TX < 10th percentile	days
TX90	Warm days, when TX < 90th percentile	days
WSDL	Annual count of days with at least 6 consecutive days when TX > 90th percentile	days
TMx	Warmest night, the highest TM	°C
TMm	Coldest night, the lowest TM	°C
TM10	Cold nights Days, when TM < 10th percentile	days
TM90	Warm nights Days, when TM > 90th percentile	days
CSDL	Annual count of days with at least 6 consecutive days when TM < 10th percentile	days

The precipitation amount with 1 mm in a day is set as the threshold for rainy days; TX denotes the daily maximum temperature; TM is the daily minimum temperature

climate-induced yield of rice and CEI can be used to explore the possible impacts of climate extremes on rice yield.

Time series analysis for CEI

In this study, the nonparametric Mann–Kendall (M–K) trend test was applied to test the trends of CEI series. In course of M–K test, the effective sample size method was used for eliminating the interference caused by serial self-correlation in the time series. Meanwhile, the Hurst exponent (*H*) was used to estimate long-term persistence of CEI series. When *H* = 0.5, it describes an independent and random time series; when $0.5 < H \leq 1$, it describes a dynamically persistent or trend reinforcing series; when $0 < H < 0.5$, it describes an anti-persistent or a mean reverting system (Shi et al. 2015). In addition, segmented regression with constraints method developed by Shao and Campbell (2002) was employed to detect both shift trends and step changes in CEI series. Further, the continuous wavelet transform (CWT) analysis, a mathematical tool to determine the most important cycles in the time series, was used for CEI series. The concept and procedure of CWT can be found at <http://paos.colorado.edu/research/wavelets/>.

Goodness of fitting tests

In the study, EasyFit professional software (version 5.4) (<http://www.mathwave.com>) was used to determine the fitting probability distribution function (PDF) of CEI series. EasyFit is a data analysis program which is commonly used in simulation application that enables the fitting PDF to the sample data, select the optimal model and to make better decisions (Atroosh and Mustafa 2012). The Kolmogorov–Smirnov (K–S) test offered by EasyFit can be considered the most widely used goodness of fit test, which employed to choose the optimal fitting probability distribution of CEI series at 5% level of significance.

Results

Climatic regionalization

At the 52 stations of Jiangsu, the multiannual mean values of 18 CEI in rice-growing period were firstly computed. Then, we applied the PCA to the 52×18 matrix composed of the average. In view of the higher variance contribution and eigenvalues of the first three principal components (PC), the three leading PC were screened (Table 2). According to the higher values of PC loading listed in Table 2, PC1 mainly denotes Dr (Number of rainy days), D25 (large precipitation days), CWD (the longest consecutive rainy days), TXm (the lowest TX), WSDL (total days of continuous

Table 2 Loading, eigenvalues, explained variances and cumulative variances calculated from applying PCA to 18 CEI

	Loading of principal components (PC) on CEI															Percentage of explained variance (%)		Cumulative percentage of explained variance (%)				
	TP	DR	D25	D50	MP1d	MP7d	CWD	P95	TXx	TXm	TX10	TX90	WSDL	TMx	TMm	TM10	TM90	CSDL				
PC1	0.53	0.96	0.65	-0.38	-0.45	-0.12	0.61	0.28	0.00	0.93	-0.47	-0.12	0.86	0.69	0.91	-0.16	-0.50	-0.12				
PC2	0.76	-0.03	0.16	0.86	0.81	0.91	0.22	0.86	-0.41	-0.18	0.24	-0.06	-0.05	-0.28	-0.27	0.03	0.30	-0.18				
PC3	-0.37	-0.16	-0.28	-0.26	-0.13	-0.28	-0.29	-0.32	0.88	-0.07	0.41	0.17	-0.07	0.47	0.04	0.05	-0.14	0.89				
	Eigenvalue															Percentage of explained variance (%)		Cumulative percentage of explained variance (%)				
PC1	5.91															32.85		32.85				
PC2	4.22															23.46		56.31				
PC3	1.82															14.14		70.46				

Loading values greater than 0.6 are in italics

high-temperature events), TMx (the highest TM) and TMm (the lowest TM); PC2 mainly denotes TP (total precipitation), D50 (rainstorm days), MP1d (Maximum 1-day precipitation) and MP7d (Maximum 7-day precipitation) and P95 [precipitation due to very wet days (> 95th percentile)]; PC3 mainly denotes TXx (the highest TX) and CSDL (total days of continuous low-temperature events).

The principal component scores (PCS) at each station are interpolated in Fig. 2, which visually shows the spatial distribution of climate extremes. The PCS-1, shown in Fig. 2a, shows positive values in the south. This means that the southern area of Jiangsu was characterized by the more rainy days and the higher daily temperature. As shown in Fig. 2b, the spatial pattern of PC-2 indicates that most of southern area had the higher-intensity extreme precipitation events. The high positive values of PC-3 in the west of Jiangsu show that there occurred the higher maximum values of daily temperature. Further, K-means cluster analysis was performed on the PCS-1, PCS-2, and PCS-3 in each

station. According to the results in Fig. 3a, six climatic subregions were identified as follows: Region I (westernmost Jiangsu), Region II (northwest Jiangsu), Region III (north Jiangsu), Region IV (southwest Jiangsu), Region V (south Jiangsu), Region VI (southeast corner of Jiangsu) (Fig. 3b). The multiannual mean values of 18 CEI in six subregions are listed in Fig. 4a, and they are well agreed with the spatial distribution of PCS.

Changing trends of CEI in different subregions

The Mann–Kendall test was applied to CEI series in different subregions (Fig. 4b). On the whole, the changing trends of precipitation-related indices (PI) in Jiangsu were not significant. As for TP, the three subregions in the northern area had weak decreasing trends, but the other subregions in the southern area had weak increasing trends. The rainy days in Jiangsu were dominated by a decreasing tendency, which was mainly reflected by the weak decrease in Dr and

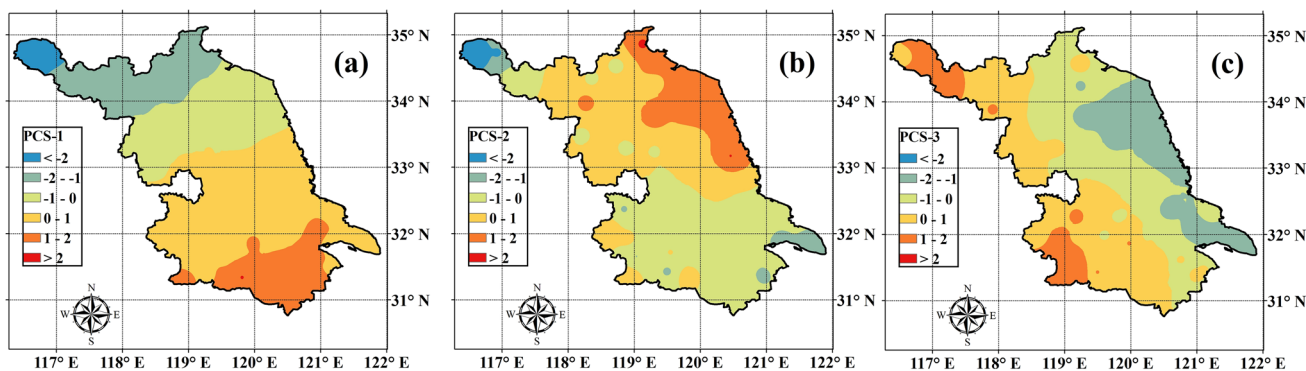


Fig. 2 Spatial distribution of principal component scores (PCS) across Jiangsu

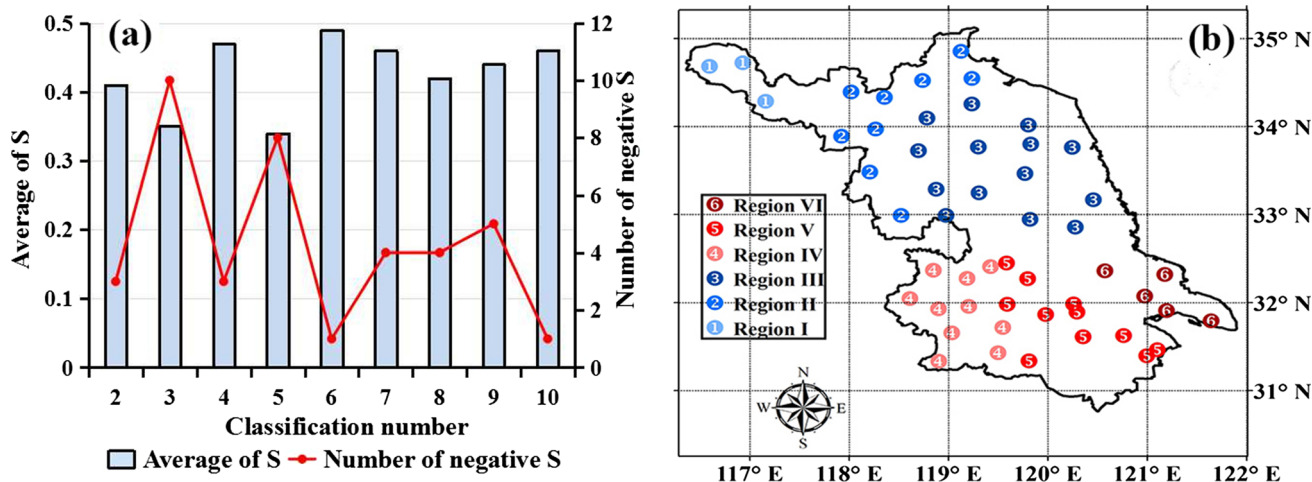


Fig. 3 Climatic regionalization based on PCS in Jiangsu (a K-means cluster analysis for PCS in all stations; b six subregions with different characteristics of climate extremes)

(a)	Region I	Region II	Region III	Region IV	Region V	Region VI	(b)	Region I	Region II	Region III	Region IV	Region V	Region VI
TP	628.43	723.14	747.39	729.31	732.62	719.57	TP	-0.53	-0.42	-0.21	0.28	0.62	0.53
DR	37.77	41.99	44.43	46.77	48.03	47.71	DR	-1.31	-1.81	-1.17	-0.74	-1.05	-0.43
D25	5.21	5.57	5.92	5.75	6.08	5.88	D25	-0.46	-1.36	-0.68	-0.11	-0.43	0.14
D50	2.77	3.40	3.38	2.96	2.82	2.80	D50	0.06	0.55	0.56	0.75	2.23	0.58
MP1d	95.89	104.24	101.26	96.13	94.10	92.74	MP1d	-0.62	0.64	0.12	1.03	1.97	1.10
MP7d	159.51	183.62	187.00	173.60	171.20	167.11	MP7d	-1.66	0.56	0.28	1.10	1.60	1.52
CWD	4.63	4.96	5.03	5.01	5.03	5.12	CWD	-0.71	-0.57	0.51	-0.99	-1.40	-0.13
P95	157.95	183.27	185.77	181.09	181.56	178.34	P95	-1.25	-0.09	0.00	0.50	0.97	0.54
TXx	37.38	36.71	36.05	37.03	36.75	36.18	TXx	0.32	0.38	1.46	2.60	4.17	3.35
TXm	13.55	14.06	14.51	15.13	15.27	15.29	TXm	1.07	1.53	1.56	1.85	2.66	2.77
TX10	17.75	17.72	17.67	17.71	17.60	17.58	TX10	0.01	-0.64	0.18	0.80	-0.05	0.55
TX90	17.56	17.45	17.44	17.43	17.46	17.36	TX90	-0.76	0.51	0.54	3.12	0.43	-0.04
WSDL	5.21	5.57	5.92	5.75	6.08	5.88	WSDL	-0.46	-1.36	-0.68	-0.11	-0.43	0.14
TMx	27.61	27.63	27.76	28.38	28.47	27.74	TMx	3.56	2.34	2.08	3.44	4.13	2.67
TMm	3.15	3.86	4.80	6.05	6.82	6.36	TMm	3.47	3.41	3.05	3.99	4.28	3.49
TM10	17.71	17.66	17.68	17.67	17.63	17.63	TM10	1.24	0.34	1.39	-0.86	-0.12	-2.08
TM90	17.40	17.40	17.46	17.21	17.22	17.20	TM90	0.10	1.01	0.84	-0.18	-0.33	0.59
CSDL	6.99	6.94	6.53	7.09	6.77	6.25	CSDL	1.10	-0.58	-0.65	-0.88	-1.12	-1.33

	Non-significant decreasing trends of CEI
	Decreasing trends of at the 10 % significance level
	Decreasing trends of at the 5 % significance level
	Non-significant increasing trends of CEI
	Increasing trends of at the 10 % significance level
	Increasing trends of at the 5 % significance level

Fig. 4 Multiannual mean values (a) and M–K test statistics (b) for CEI series in six subregions (the detail of units for each CEI in Fig. 4a is listed in Table 1)

CWD occurred in most of subregions. However, D50, MP1d, MP7d, and P95 showed weak increasing trends in most of subregions, implying the intensifying of high-intensity rainfalls in Jiangsu. Especially in Region V (south Jiangsu), D50 and MP1d had significant increasing trends. Compared to PI, the trends of temperature-related indices (TI) in Jiangsu were more significant. Especially for TMx and TMm, the increasing trends at the significant level of 5% were detected in each subregion. Similarly, TXx and TXm were increasing in each subregions, and the significant increase was observed for the three subregions in the southern area. In addition, the decrease of TM10 was found in the southern area of Jiangsu. In view of the above, it can be conclude that this province was dominated by the wetting and warming tendency during rice-growing period, especially in the southern area of Jiangsu.

Correlation between rice yield and CEI

The correlation analyses between rice yield and PI, TI in each subregion were performed by using both of first-difference method and climate-induced yield method. As shown in Fig. 5a, all the PIs were negatively correlated with rice yield, and the significant negative correlation between PI and yield could be observed in each subregion. Especially in Region IV and V, most of PI were negatively correlated with rice yield at the significance level of 1%. It was worth mentioning that different PI had different applicability for depicting

the negative impact of precipitation extremes. As to four subregions including II, III, IV, and V, all the absolute values of correlation between P95 and rice yield reached the maximum, implying that P95 should be considered as an optimal indicator for precipitation-induced rice meteorological disasters in most of Jiangsu. For Region I and VI, D50 should be considered as an optimal indicator to show precipitation extremes with the highest negative correlation. Meanwhile, the correlations calculating using climate-induced yield method are given in Fig. 5b. Overall, the results derived from climate-induced yield method were well agreed with first-difference method. However, the negative impact of PI on rice yield by using climate-induced yield method was not obvious in Region I.

In Fig. 5, both of positive and negative correlations were detected on the relationship between TI and rice yield, which implies the regional difference for the impacts of temperature extremes on rice yield. For example, the positive correlations between yield and TXm were found in Region I and IV, while the negative correlations between yield and TXm were found in the other subregions. Previous studies show that the correlations between rice yield and temperature variables vary greatly across south China; on the other hand, the topographic conditions, cropping patterns, and rice varieties in different climate zones might influence the responses of the rice yield to temperature extremes (Tao et al. 2008). However, the negative correlations between yield, and WSDL and TMm were observed in each subregions (Fig. 5a,

(a)	Region I	Region II	Region III	Region IV	Region V	Region VI		(b)	Region I	Region II	Region III	Region IV	Region V	Region VI
TP	-0.37	-0.44	-0.37	-0.42	-0.41	-0.32		TP	-0.20	-0.32	-0.36	-0.44	-0.41	-0.29
DR	-0.28	-0.45	-0.33	-0.36	-0.42	-0.25		DR	-0.20	-0.39	-0.39	-0.43	-0.48	-0.30
D25	-0.15	-0.48	-0.31	-0.16	-0.20	-0.09		D25	-0.02	-0.26	-0.23	-0.18	-0.19	-0.12
D50	-0.38	-0.25	-0.30	-0.40	-0.42	-0.41		D50	-0.26	-0.22	-0.30	-0.39	-0.38	-0.40
MP1d	-0.12	-0.24	-0.17	-0.44	-0.47	-0.27		MP1d	-0.12	-0.23	-0.26	-0.38	-0.40	-0.20
MP7d	-0.18	-0.26	-0.27	-0.39	-0.41	-0.28		MP7d	-0.07	-0.16	-0.25	-0.37	-0.37	-0.21
CWD	-0.15	-0.31	-0.45	-0.44	-0.42	-0.22		CWD	0.05	-0.04	-0.29	-0.47	-0.44	-0.29
P95	-0.27	-0.50	-0.50	-0.51	-0.50	-0.33		P95	-0.18	-0.42	-0.41	-0.52	-0.50	-0.31
TXx	-0.09	0.02	-0.03	0.02	0.27	0.19		TXx	-0.01	0.06	-0.02	0.07	0.29	0.21
TXm	0.10	-0.13	-0.25	0.17	-0.01	-0.06		TXm	0.10	-0.16	-0.16	0.12	-0.07	0.05
TX10	-0.05	0.09	0.01	-0.01	0.11	-0.18		TX10	-0.05	-0.03	0.07	0.01	0.05	-0.10
TX90	-0.32	-0.13	0.02	0.13	0.12	-0.15		TX90	-0.14	-0.05	-0.11	-0.02	0.13	-0.18
WSDL	-0.15	-0.48	-0.31	-0.16	-0.20	-0.09		WSDL	-0.02	-0.26	-0.23	-0.18	-0.19	-0.12
TMx	-0.17	-0.11	-0.15	-0.13	0.11	0.11		TMx	-0.02	-0.15	-0.18	-0.12	0.11	0.13
TMm	-0.31	-0.06	-0.21	-0.01	-0.08	-0.19		TMm	-0.24	-0.08	-0.17	-0.10	-0.12	-0.10
TM10	0.19	0.26	0.05	-0.13	0.12	0.13		TM10	0.24	0.19	0.05	-0.08	0.11	0.04
TM90	-0.03	-0.28	0.03	0.10	-0.13	0.16		TM90	-0.04	-0.28	0.02	0.07	0.00	0.08
CSDL	-0.02	0.05	0.12	0.01	-0.07	0.18		CSDL	-0.08	0.14	0.22	0.03	-0.06	0.22

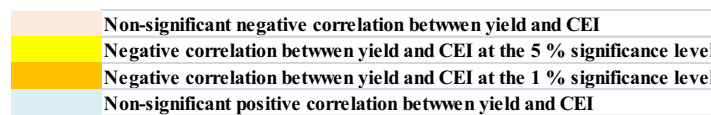


Fig. 5 Correlation between rice yield and CEI in all subregions (a correlation computed using first-different method; b correlation computed using climate-induced yield method)

b). This may indicate that the unfavorable influence of longer continuous high-temperature events and higher night minimum temperature on rice yield were common across Jiangsu. In general, the impact of temperature extremes on rice yield was not obvious, which was reflected by the lower correlations between yield and TI. However, it is worth noting that the significant negative correlations between yield and some indicators characterizing high-temperature events (TX90 and WSDL) were observed in Region I, II, and III (Fig. 5a), suggesting that the rice growing in the northern area of Jiangsu might be more sensitive to heat stress.

Temporal variations of P95 in most of Jiangsu

In view of the most notable negative impacts of P95 on rice yield, the temporal variations of P95 in four key subregions were discussed (Fig. 6). According to the different Hurst exponent values listed in Fig. 6, the temporal evolution of P95 in Region III was characterized by long memory, while P95 in Region II, IV, and V showed the anti-persistent changing pattern. The coefficient of variation (CV) for P95 series was ranged from 27.07 to 32.30%, and the CV in Region IV was the biggest. Additionally, the segmented regression was employed to detect the shift trend. P95 in Region II, III, and IV had a W-shape changing pattern (decreasing–increasing–decreasing–increasing), while P95 in Region V showed a relatively gentle inter-annual fluctuation. It is noteworthy that an increase of P95 since 1990s was observed in each subregions. Furthermore, the continuous wavelet transform (CWT) was used for capturing the

oscillatory features of P95 in four subregions. As displayed in Fig. 7, a 2–4 year periodical feature was noticeable in each P95 series over the province.

Identifying the best probability distribution for P95 series can be beneficial for further understanding of the unique and complex characteristics of precipitation extremes. Figure 8a shows the Kolmogorov–Smirnov test (KS) for evaluating the goodness of fit according to different probability distributions for P95. Obviously, the Gen Extreme Value (GEV) distribution provided the best estimation with the smallest KS value for P95 series in each subregion. On the basis of the best fit model, Fig. 8b illustrates the outcomes of P95 with return periods of 2, 5, 10, 15, 20, 30, 40, 50, 100 years, respectively. Results indicated that the values of P95 were increasing nonlinearly as corresponding return periods, and the higher increasing rates of CEI were mainly observed when the return periods were less than 20 years. The values of P95 in Region IV and V were obviously larger than Region II and III when the corresponding return periods were greater than 20 years, which implies the higher destructiveness of precipitation-related rice meteorological disasters in the southern area.

Conclusions and discussions

A total of 18 CEI of rice-growing period were constructed in Jiangsu province. The regional variations of climate extremes and their possible impacts on rice yield were discussed. The main findings were as follows:

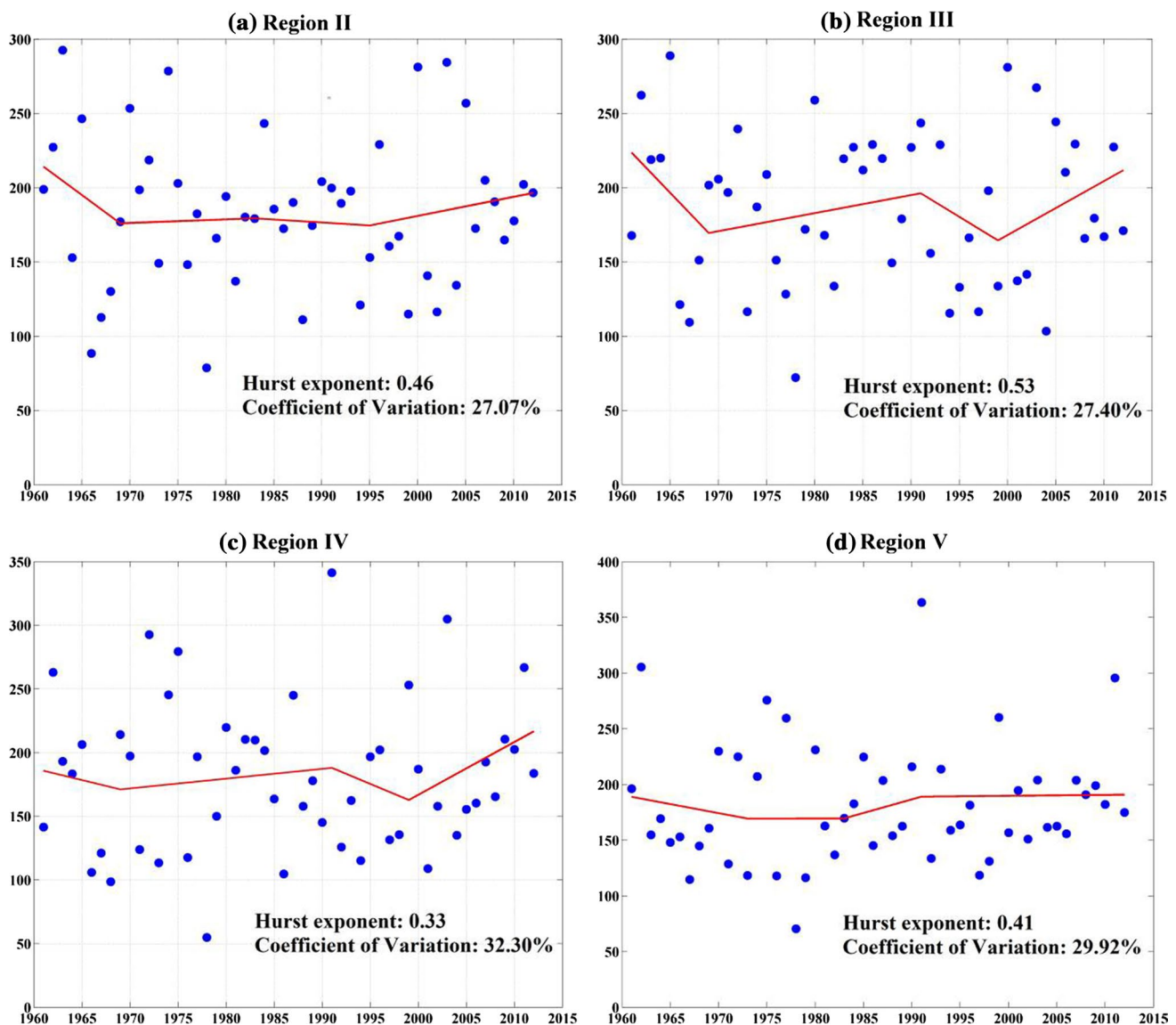


Fig. 6 Hurst exponent, coefficient of variation, and segmented regression for P95 series in four key subregions (the blue dot denotes the observed values of P95; solid red line denotes the trend by segmented regression)

Based on PCA, the obvious spatial variations of climate extremes were observed in Jiangsu. Overall, the northern area of Jiangsu had more severe precipitation extremes. Located in the climatic and sea-land transition zone, the northern area was mainly influenced by the various weather systems including west-pacific subtropical high (WPSH), Meiyu front, westerly trough and typhoon along the northeastern coast (Xiao et al. 2006). Thus, the northern area had frequent severe convection weather and unstable atmospheric structure, which caused the higher frequency of rain-storm events. Being dominated by subtropical monsoon climate, the southern area had the higher temperature and the more rainy days compared to the northern area. In addition, the higher daily maximum temperature was observed in

the western area, which was mainly attributed to the strong dominance of WPSH during the west-extending period (Huang et al. 2017). Due to the obvious regional difference of climate extremes, Jiangsu could be divided into six subregions using clustering analysis, i.e., westernmost, northwest, north, southwest, south, southeast corner, respectively.

By using the Mann–Kendall trend test for CEI in each subregion, the intensifying of high-intensity rainfalls were found in Jiangsu. In the recent 20 years, the increasing northeasterly wind tendency over central and eastern China was weakening the southwesterly summer monsoon, limiting its northward extension, and the long-term retention of summer rain belt over the mid-lower Yangtze River basin tends to produce heavier rainfalls (Wang and Zhou

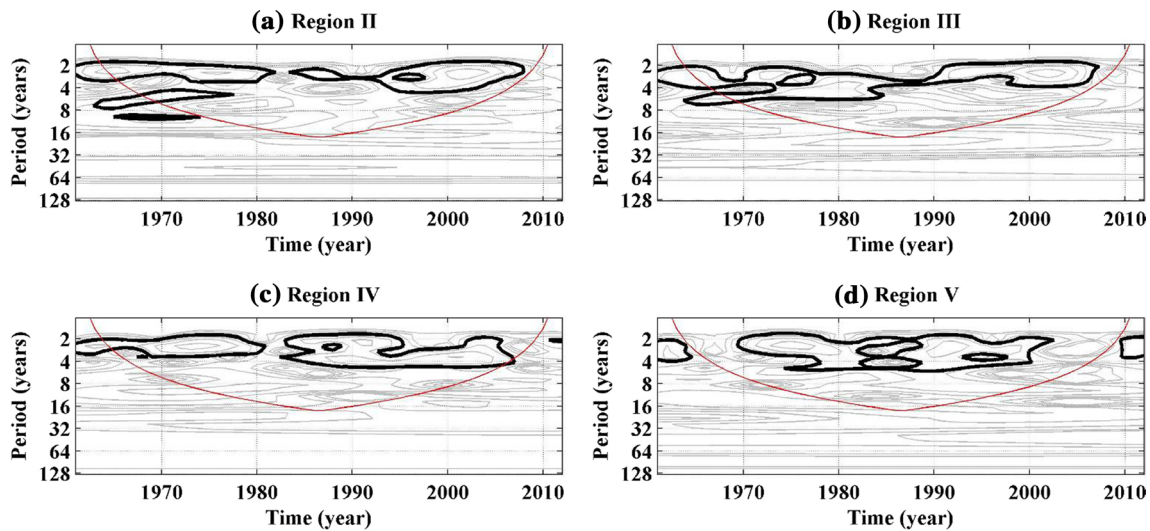


Fig. 7 Wavelet power spectrum of P95 in four subregions (the 5% significance level against red noise is shown as thick black contours, and the cone of influence (COI) where edge effects might distort the picture is shown as the U-shaped curves)

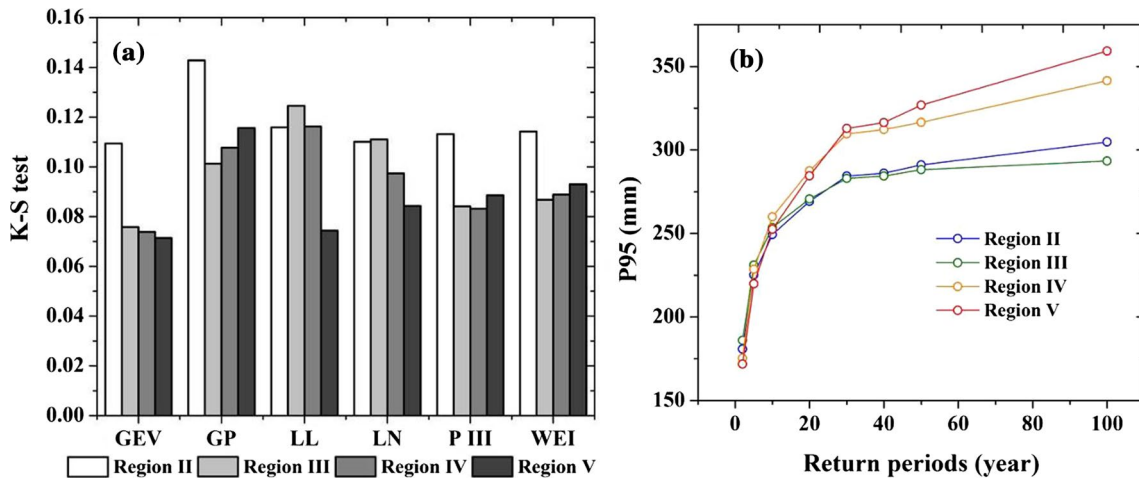


Fig. 8 Goodness of fitting results by K-S Test for P95 series (*GEV* generalized extreme value, *GP* generalized pareto, *LL* Log-Logistic, *LN* log-normal, *P III* Pearson III, *WEI* weibull) (a) and outcome of best fitted distribution for CEI series in different return periods (b)

2005). Also, increasing geopotential height over Mongolia and northern China, the South China Sea and west Pacific regions has prevented the northward propagation of the vapor flux, was intensifying the precipitation extremes (You et al. 2011). Moreover, the strong increase in daily maximum and minimum temperature was detected. These might be attributed to the strength of western Pacific subtropical high and the decrease in sea ice of Kaka Sea in summer (Huang et al. 2017; Wang et al. 2015). Compared to the northern area, the wetting and warming tendency in the southern area seemed more significant. Due to the rapider urbanization, the more complex atmospheric components, stronger heat island effect and more prominent rain

island effect in the southern area would further intensify the climate changes (Xia et al. 2015).

Previous studies noted that the heat stress was one of meteorological disasters for rice growing in the mid-lower Yangtze Basin (Bao et al. 2012). Similarly, we found that a negative correlation between rice yield and WSDL existed in each subregion of Jiangsu. Especially in westernmost, northwest, and north Jiangsu, rice yield were negatively correlated with high-temperature indices significantly, implying the northern area of Jiangsu should be classified as sensitive region for rice heat stress. Heat stress associated with dry spell (consecutive rainless periods) often caused the decline of rice yields in the mid-lower Yangtze Basin;

therefore, the different responses of rice yield to heat stress were mainly determined by the drought condition and irrigation water availability in different degrees (Shuai et al. 2013). Compared to the northern area, the more rainy days and better-suited irrigation system in the southern area were more favorable for rice growth (Wu et al. 2015). Thus, the negative impacts of heat stress on rice yield in the southern area of Jiangsu were not obvious.

Most of all, we found that the strong and negative correlations existed between rice yield and PI in each subregions. Especially in four subregions including northwest, and north, southwest and south Jiangsu, the correlation between rice yield and P95 were all smaller than -0.5 . P95, a precipitation indicator calculated using percentile threshold method, had the better applicability for screening the precipitation extremes and overcoming the regional differences (Liu et al. 2016b). Due to the high-intensity rainfalls, lower elevation and larger drainage density, Jiangsu province was the high hazard region for flood disaster (Wu et al. 2015). The waterlogging and floods caused by extreme precipitation events would reduce rice yield directly; therefore, the negative correlations between rice yield and P95 were most significant in most of Jiangsu. In view of this, the monitoring and forecasting of P95 should be used to access the rice yield losses caused by the meteorological disasters, and it also could be used as a key indicator for the risk regionalization. More worrying, the significant increase of P95 was observed in most of Jiangsu after 1990s, which would bring huge risks to rice growing.

Acknowledgements This paper was mainly supported by China Special Fund for Meteorological Research in the Public Interest (Major projects) (GYHY201506001-6), Jiangsu Province Science Fund for Excellent Young Scholars (BK20170102), Open Fund of Jiangsu Key Laboratory of Agricultural Meteorology/Nanjing University of Information Science and Technology (JKLAM1603, JKLAM1604), Natural Science Foundation of Jiangsu Higher Education Institutions of China (16KJB170008), Open Research Fund of Key Laboratory of Agrometeorological Support and Applied Technique/China Meteorological Administration (AMF201507, AMF201608).

References

- Ara I, Lewis M, Ostendorf B (2016) Spatio-temporal analysis of the impact of climate, cropping intensity and means of irrigation: an assessment on rice yield determinants in Bangladesh. *Agric Food Secur* 5(1):12
- Arshad M, Amjath-Babu TS, Krupnik TJ et al (2017) Climate variability and yield risk in South Asia's rice-wheat systems: emerging evidence from Pakistan. *Paddy Water Environ* 15:249
- Atroosh KB, Mustafa AT (2012) An estimation of the probability distribution of Wadi Bana flow in the Abyan Delta of Yemen. *J Agric Sci* 4(6):80
- Bao Y, Liu W, Gao P, Shen S (2012) Study on characteristics of rice heat damages in Jiangsu province under the background of climate warming and its influence on rice yield. *Chin J Agrometeorol* 33:289–296 (in Chinese with English abstract)
- EI-Maayar M, Lange MA (2013) A methodology to infer crop yield response to climate variability and change using long-term observations. *Atmosphere* 4:365–382
- Huang J, Zhan F, Xue Y, Li Q (2016a) Recent changes of extreme dryness/wetness pattern and its possible impact on rice productivity in Jiangsu province, southeast China. *Nat Hazards*. <https://doi.org/10.1007/s11069-016-2529-0>
- Huang J, Chen X, Zhou L et al (2016b) Statistical analysis of the relationship between climate-induced maize yield and rainy-season precipitation across Inner Mongolia, North China. *Theor Appl Climatol*. <https://doi.org/10.1007/s00704-016-1839-1>
- Huang J, Zhan F, Xue Y et al (2017) Recent changes of rice heat stress in Jiangxi province, southeast China. *Int J Biometeorol* 61(4):623–633
- Kaufman L, Rousseeuw P (1990) Finding groups in data: an introduction to cluster analysis. Wiley Press, New York
- Lee MH, Ho CH, Kim J et al (2012) Assessment of the changes in extreme vulnerability over East Asia due to global warming. *Clim Change* 113(2):301–321
- Liu Y, Xiao J, Ju W et al (2016a) Recent trends in vegetation greenness in China significantly altered annual evapotranspiration and water yield. *Environ Res Lett* 11(9):094010
- Liu B, Chen X, Chen J et al (2016b) Impacts of different threshold definition methods on analyzing temporal-spatial features of extreme precipitation in the Pearl River Basin. *Stoch Environ Res Risk Assess*. <https://doi.org/10.1007/s00477-016-1284-9>
- Quan C, Jing YS, Tan KY (2013) Progress in research of impacts of climate change on yield of three major grain crops. *Chin Agric Sci Bull* 29(32):361–367 (in Chinese with English abstract)
- Revadekar JV, Preethi B (2012) Statistical analysis of the relationship between summer monsoon precipitation extremes and foodgrain yield over India. *Int J Climatol* 32(3):419–429
- Rummukainen M (2013) Climate change: changing means and changing extremes. *Clim Change* 121(1):3–13
- Sawano S, Hasegawa T, Ishigooka Y et al (2015) Effects of nitrogen input and climate trends on provincial rice yields in China between 1961 and 2003: quantitative evaluation using a crop model. *Paddy Water Environ* 13:529
- Shao QX, Campbell NA (2002) Modeling trends in groundwater levels by segmented regression with constraints. *Aust N Z J Stat* 44:129–141
- Shi P, Wu M, Qu S et al (2015) Spatial distribution and temporal trends in precipitation concentration indices for the Southwest China. *Water Resour Manag* 29(11):3941–3955
- Shuai J, Zhang Z, Liu X et al (2013) Increasing concentrations of aerosols offset the benefits of climate warming on rice yields during 1980–2008 in Jiangsu province, China. *Reg Environ Change* 13(2):287–297
- Sönmez İ, Kömüştü AÜ (2011) Reclassification of rainfall regions of Turkey by K-means methodology and their temporal variability in relation to North Atlantic Oscillation (NAO). *Theor Appl Climatol* 106(3–4):499–510
- Sun S, Chen H, Ju W et al (2013) Effects of climate change on annual streamflow using climate elasticity in Poyang Lake Basin, China. *Theor Appl Climatol* 112(1–2):169–183
- Sun SL, Sun G, Caldwell P et al (2015) Drought impacts on ecosystem functions of the U.S. National Forests and grasslands: part II assessment results and management implications. *For Ecol Manag* 353:269–279
- Tao F, Yokozawa M, Liu J et al (2008) Climate-crop yield relationships at provincial scales in China and the impacts of recent climate trends. *Clim Res* 38(1):83–94
- Wang XL, Feng Y (2013) RHTestsV4 user manual. Climate Research Division, ASTD

- Wang Y, Zhou L (2005) Observed trends in extreme precipitation events in China during 1961–2001 and the associated changes in large-scale circulation. *Geophys Res Lett* 32(9):L09707
- Wang D, He J, Qi L et al (2015) Temperature characteristics of Eurasia in autumn and winter and its cause under global warming mitigation. *J Meteorol Sci* 35(5):534–542 (**in Chinese with English abstract**)
- Wang QX, Wang MB, Fan XH et al (2016) Trends of temperature and precipitation extremes in the Loess Plateau Region of China, 1961–2010. *Theor Appl Climatol*. <https://doi.org/10.1007/s00704-016-1820-z>
- Wu Y, Zhou P, Zhang Y et al (2015) Integrated flood risk assessment and zonation method: a case study in Huaihe River basin, China. *Nat Hazards* 78:635–651
- Xia L, Zhang Q, Ning Sun et al (2015) Climate change characteristics in Jiangsu province, 1960–2012. *J Glaciol Geocryol* 37(6):1480–1489 (**in Chinese with English abstract**)
- Xiao H, Jiang AJ, Shen Z et al (2006) The space-time distribution characters of maximum diurnal precipitation in Jiangsu province and the statistic assimilation. *Sci Meteorol Sin* 26(2):177–182 (**in Chinese with English abstract**)
- Yang L, Qin Z, Tu L (2015) Responses of rice yields in different rice-cropping systems to climate variables in the middle and lower reaches of the Yangtze River, China. *Food Secur* 7(5):951–963
- You Q, Kang S, Aguilar E et al (2011) Changes in daily climate extremes in China and their connection to the large scale atmospheric circulation during 1961–2003. *Clim Dyn* 36:11–12